[2]Davis, R. T., "A Procedure for Solving the Compressible Interacting Boundary Layer Equations for Subsonic and Supersonic Flows," AIAA Paper 84-1614, 1984.

[3]Smith, A. M. O., and Gamberoni, N., "Transition Pressure Gradient, and Stability Theory," Douglas Aircraft Co. Rept. ES 25388, El Segundo, CA, 1956.

[4]Jaffe, N. A., Okamura, T. T., and Smith, A. M. O., "Determination of Spatial Amplification Factors and Their Application to Predicting Transition," *AIAA Journal*, Vol. 8, No. 2, 1970, pp. 301–308.

[5]Masad, J. A., and Iyer, V., "Transition Prediction and Control in Subsonic Flow over a Hump," *Physics of Fluids*, Vol. 6, No. 1, 1994, pp. 313–327.

[6]Fage, A., "The Smallest Size of Spanwise Surface Corrugation Which Affect Boundary Layer Transition on an Airfoil," British Aeronautical Research Council, 2120, 1943.

[7]Carmichael, B. H., "Surface Waviness Criteria for Swept and Unswept Laminar Suction Wings," Northrop Aircraft Rept. NOR-59-438 (BLC-123), 1957.

[8]Larson, H. K., and Keating, S. J., "Transition Reynolds Numbers of Separated Flows at Supersonic Speeds," NASA TN D-349, 1960.

[9]Chapman, D. R., Kuehn, D. M., and Larson, H. K., "Investigation of Separated Flows in Supersonic and Subsonic Streams with Emphasis on the Effect of Transition," NACA Rept. 1356, 1958.

[10]Van Driest, E. R., and Boison, J. C., "Experiments in Boundary-Layer Transition at Supersonic Speeds," *Journal of the Aeronautical Sciences*, Vol. 24, 1957, pp. 885–899.

[11]Lin, C. C., "The Theory of Hydrodynamic Stability," Cambridge Univ. Press, Cambridge, England, UK, 1955.

[12]Coles, D., "Measurements of Turbulent Friction on a Smooth Flat Plate in Supersonic Flows," *Journal of the Aeronautical Sciences*, Vol. 21, No. 7, 1954, pp. 433–448.

[13]Fage, A., and Preston, J. H., "On Transition from Laminar to Turbulent Flow in the Boundary Layer," *Proceedings of the Royal Society of London*, Vol. 178, 1941, pp. 201–227.

Whistler-Driven, Electron-Cyclotron-Resonance-Heated Thruster: Experimental Status

B. W. Stallard* and E. B. Hooper†
Lawrence Livermore National Laboratory, Livermore, California 94551
and
J. L. Power‡
NASA Lewis Research Center, Cleveland, Ohio 44135

Introduction

EXPANSION of an electron-cyclotron-resonance- (ECR) heated plasma in a magnetic nozzle offers several potential advantages over other plasma thrusters for generating high specific impulse I_{sp}. The use of microwaves eliminates electrodes, a primary life-limiting component for most plasma devices; space charge ion acceleration eliminates the acceleration grid problems of ion thrusters; and wall interactions are less than other plasma thrusters, reducing energy and particle losses and the sputtering of wall material. In addition, an ECR thruster can deliver very high-power density and offers the possibility of variable I_{sp} through control of the plasma potential. In this Note we summarize for the propulsion community the experimental status of an approach[1–3] proposed to overcome limitations of previous ECR thrusters,[4–7] especially plasma density limited by microwave cutoff at frequencies below the plasma frequency, significant power losses to atomic radiation, and plasma recycling at an interior rear wall in contact along the magnetic field.

Received June 4, 1995; revision received Dec. 20, 1995; accepted for publication Feb. 6, 1996.

*Physicist, Magnetic Fusion Energy, Energy Directorate.
†Assistant Deputy Associate Director, Magnetic Fusion Energy, Energy Directorate. Member AIAA.
‡Aerospace Engineer, M/S 301-3. Member AIAA.

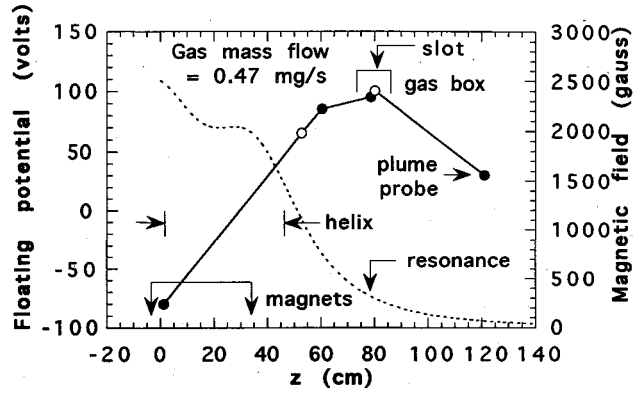

Fig. 1 Magnetic field (dashed line) and floating potentials along the plasma. Shown are potential measurements on axis (solid points) and edge (open points). Gas propellant is injected through the slot into a nine-section gas box.

In our experiment several new features are used. First, whistler waves are excited in the plasma at a magnetic field strength B higher than resonance given by $B_{res} = (m_e/e)2\pi f$, where f is the microwave frequency, and m_e and e are the electron mass and charge, respectively. The wave frequency satisfies $f < f_{ce}, f_{pe}$, where $f_{ce} = eB/2\pi m_e$ is the local electron cyclotron frequency (typically ~5 GHz), $f_{pe} = (1/2\pi)\sqrt{e^2 n_e/\varepsilon_0 m_e}$ is the plasma frequency (typically ~6 GHz), n_e is the electron density, and ε_0 is the free space permittivity. The whistler wave is the only electron wave that propagates at arbitrarily high densities.[8] Second, the resonance is located on the side of a magnetic hill below the peak field, as shown in Fig. 1. This reduces power flow up the hill to the rear boundary because the magnetic flux tube area decreases as the field increases. Third, hydrogen is injected in a gas box at a field below the resonance, where it is ionized by the heated electrons. Calculations predict that the magnetic forces caused by the anisotropic ECR electron distribution can greatly reduce energy losses up the hill.[3,9] Fourth, the use of hydrogen or deuterium minimizes energy losses from atomic line radiation.

Floating potentials $\geq$100 V are generated in the plasma as predicted[9] and an ion flux down the magnetic field is generated with energy characteristic of these potentials. We have also measured the excited whistler waves and their propagation and absorption in overdense plasma at the resonance. Observed discharge particle and energy efficiencies are lower than expected, probably because the injected gas is not fully ionized and losses to the rear wall are greater than predicted. Modifications to achieve high efficiencies are suggested.

Description of the Experiment

The apparatus is shown in Fig. 2. Microwaves at f = 915 MHz (B_{res} = 0.0327 T) and power up to 20 kW (30–100 ms pulse length) are coupled from a bihelical antenna to a plasma column at a magnetic field strength typically near 0.21 T. The antenna is in air, outside a 4.9-cm-i.d.-fused silica tube vacuum envelope to prevent electrical breakdown problems.[3] The axial magnetic field profile, shown in Fig. 1, is generated by two solenoidal magnets located at z = −4.3 and 34.4 cm, with mean conductor radii of 27.9 cm.[3] The magnitude, axial profile, and resonance location are varied by changing magnet currents. The resonance is between the wave-launching column and the gas box, slightly upfield of the gas box slot, as

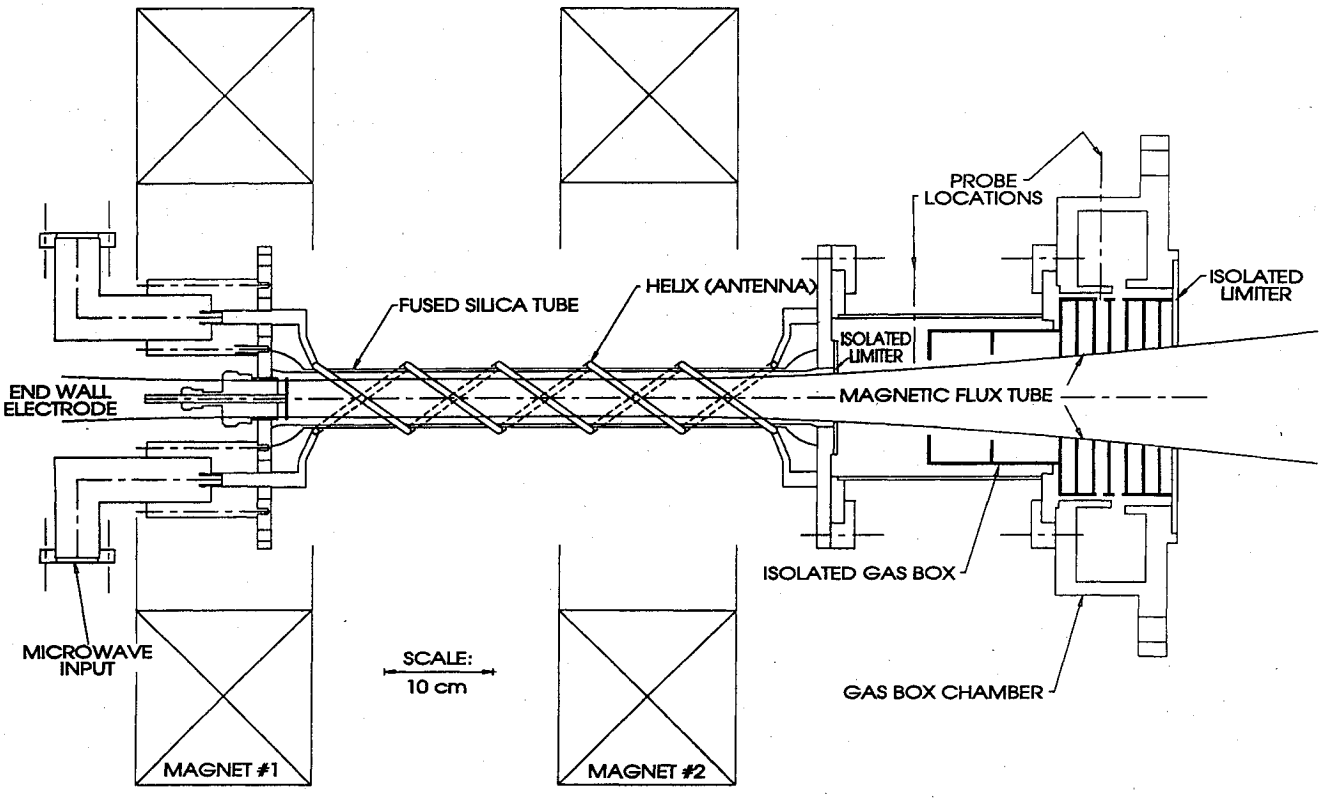

Fig. 2 Sketch of thruster geometry showing magnets, helix rf coupler, and propellant feed region, as described in the text.

in the computations.[3,9] To minimize bombardment of the silica, an electrically isolated stainless-steel limiter at the low field end of the tube limits the plasma diameter to 4.4 cm. A second isolated limiter, bounding the same magnetic flux tube, is placed at the low field end of the gas box. An isolated stainless-steel disk at the high field end terminates the discharge.

Hydrogen is injected into a gas box using pulsed, piezoelectric valves. The gas box is segmented, to reduce gas loss before plasma ionization, and it is also isolated, so that there are no electrically grounded surfaces contacting the plasma in the discharge region. Ground is determined where the magnetic field lines intersect the downstream vacuum pumping vessel.

Diagnostics include langmuir probes at the end wall ($z = 0$), between the antenna and gas box ($z = 59$ cm), and in the gas box ($z = 77$ cm). These probes also measure the microwave electric field or are replaced by rf loop probes to measure the microwave magnetic field. The electric potentials of the various surfaces and limiters, biased to draw zero current (floating potential) are also measured. Exterior to the thruster, 35 cm downstream from the end of the gas box, is a gridded ion detector (plume probe) to measure the ion flux as a function of energy, allowing us to characterize the ion beam.

Results and Discussion

Measured plasma densities and ion fluxes for pulsed operation demonstrate that the plasma reaches equilibrium in 30–40 ms. Detailed discharge characteristics depend on the operating point. At low propellant flow rates, ≤0.47 mg/s (<4 Torr-l/s), and high power, ≥15 kW, the electron density n_e and temperature T_e are about $2–3 \times 10^{11}$ cm^{-3} and 10–20 eV, respectively. The gas is not fully ionized, with the consequences discussed later. Figure 1 shows a typical time-averaged, floating potential axial profile, measured using langmuir probes on the axis, the floating limiters, and the end wall. The on-axis probes and edge limiters have similar potentials.

The ion flux measured by the plume probe is shown in Fig. 3. When it is moved transversely, we find that the ion beam is confined to the flux tube that passes through the final gas box limiter. The magnetic field curvature between the limiter

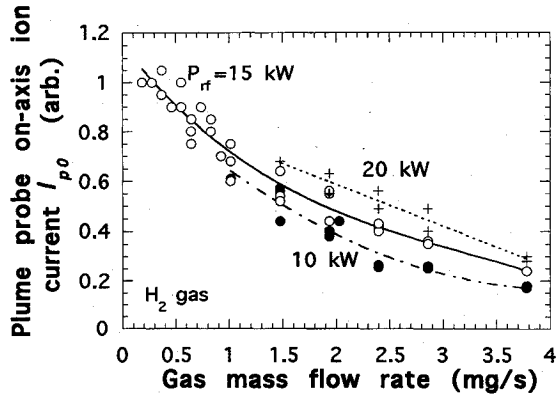

Fig. 3 Ion current to the plume probe, showing increase with reduced gas injection and increased microwave power.

and probe is small because large coils are used in the experiment. This experiment was not designed for significant plasma plume separation from the magnetic field. With concentration of the beam near the magnetic axis, theory predicts that a careful magnetic field design is required.[10]

As the gas injection rate decreases and microwave power increases, n_e and T_e increase. Thus, Fig. 3 shows the on-axis plume probe ion current I_{p0} increasing by about a factor of 4 as the gas flow decreased from 3.5 to <0.6 mg/s: effective ionization increases as the gas injection decreases. The beam ions measured by the probe are accelerated by large space potentials (Fig. 1) so that $I_{p0} \sim n_i \langle\sqrt{E_i}\rangle$, where $\langle\sqrt{E_i}\rangle$ is the mean ion velocity. From the measured ion energies shown in Fig. 4, it appears that the increase in beam current as the gas flow decreases results from a modest increase in ion density and a larger increase in $\langle\sqrt{E_i}\rangle$. Ion beam energy spectra, found by sweeping the plume probe repeller voltage, are shown in Fig. 4 for low and high gas flow. The case corresponding to Fig. 1 at low gas flow has an average energy of 85 eV ($I_{sp} \approx 9 \times 10^3$ s), with a peak of at least 150 eV. The energy spread

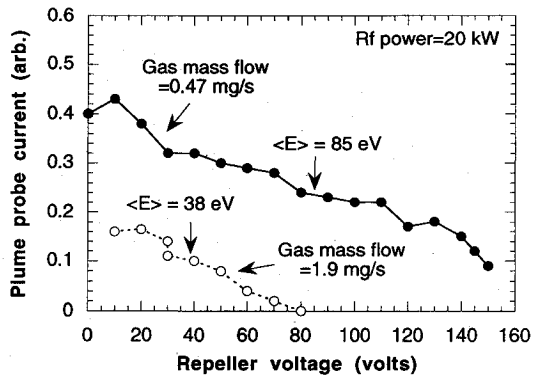

Fig. 4 Ion energy spectrum at the plume probe for low- and high-gas flows.

is probably because of charge-exchange of the expanding plasma on background gas. The peak energy is larger than the difference in average voltage from Fig. 1, as expected, because plasma potentials in Maxwellian plasmas exceed floating potentials by $\sim 0.5T_e\ \ell n(m_i/m_e)$, where m_i is the ion mass. The highest potentials are characteristic of the peak voltage fluctuations in the plasma, as discussed next.

During high-density operation ($n_e \sim 3 \times 10^{11}$ cm^{-3}), the plasma density and temperature at fields above the resonance are comparable to those below. This differs from the computational results,[9] which assume a gas ionization particle source confined to the gas box. In addition, the computations find that gas recycling from plasma striking the wall at high field is insufficient to account for similar densities above resonance and at the gas box. We conclude that neutral gas ionization occurs along the plasma column at high field; this conclusion is reasonable for our present parameters because the ionization mean-free-path is about 35 cm for neutral hydrogen molecules at room temperature. Even though this will be reduced by the energetic tail from the ECR heating, it is still too long for the gas to be fully ionized, and more energetic hydrogen atoms, characteristic of Franck–Condon neutrals or of charge-exchange neutrals, will have even longer mean-free-paths.[11]

At low gas flow the discharge exhibits large potential and density fluctuations, suggesting a bimodal operation or switching behavior that may indicate high- and low-density modes in the high field region. These fluctuations limit the lowest usable gas flow, at which the energy and particle utilization efficiencies, as estimated from gas flow rates, measured temperatures, and ion fluxes, are 1–5%.

To conclude, we hypothesize the following operational model and suggest experimental approaches to validate it with the goal of improving thruster efficiency.

1) The bimodal characteristic suggests a microwave coupling variation with density and the following scenario: At high-density wave coupling is efficient and plasma potentials develop that reduce up-field plasma flow, subsequently reducing up-field density, lowering antenna coupling and ionization in the gas box. This is supported by the computational analysis that predicts a high field density of at least a factor 3 less than in the gas box, because ECR increases the energy perpendicular to the magnetic field, thus generating a force down the field gradient.[9] The potential and density then fall. Density recovers by ionization of gas under the antenna. Efficient coupling, gas box fueling, and potentials now rise and the cycle repeats. Improvement of this coupling can best be achieved using a new antenna design that injects the power closer to, but still upfield from, the resonance. This would also minimize any nonresonant heating of plasma, further increasing the efficiency.

2) Because the plasma density in the gas box is too low to ensure full ionization of injected gas, neutral atoms can travel up the column resulting in volume ionization along the entire length. Also, gas escaping downstream from the gas box will charge exchange with the ions, broadening the energy spectrum as shown in Fig. 4. Improved ionization rate can be achieved by a weak magnetic mirror at the gas box, yielding a longer plasma residence time and higher density. The corresponding increased ionization rate will further increase the density; the goal is a large enough increase for full ionization. Achievement of full ionization and the reduction of ionization in the high field column should substantially improve both energy and particle efficiencies for this thruster concept and improve prospects for rf-powered thrusters.

Acknowledgments

This work was performed under the auspices of the U.S. Department of Energy by Lawrence Livermore National Laboratory under Contract W-7405-ENG-48 and of the NASA Lewis Research Center. We are pleased to acknowledge Walter Ferguson whose assistance in setting up the high-power microwave circuitry was essential to the success of the experiment. We also are indebted to Michael Makowski who contributed to many of the ideas and early experiments. The support of David Byers throughout the course of this experiment provided an environment in which the ideas and techniques could be developed. Our interest in the ECR approach to thrusters was triggered by discussions with Joel Sercel of the Jet Propulsion Laboratory, California Institute of Technology.

References

[1]Hooper, E. B., "Microwave-Generated Plasma Thruster," Lawrence Livermore National Lab., UCRL-ID-107211, Livermore, CA, May 1991.

[2]Hooper, E. B., Stallard, B. W., and Makowski, M. A., "Whistler Wave Driven Plasma Thruster," *10th Symposium on Space Nuclear Power and Propulsion* (Albuquerque, NM), edited by M. S. El-Genk and M. D. Hoover, American Inst. of Physics CP 271, Pt. 3, New York, 1993, pp. 1419–1424.

[3]Hooper, E. B., Ferguson, S. W., Makowski, M. A., Stallard, B. W., and Power, J. L., "Analysis and Experiments of a Whistler-Wave Plasma Thruster," *Proceedings of the 23rd International Electric Propulsion Conference* (Seattle, WA), Vol. 1, 1993, Ohio State Univ., Columbus, OH, 1993, pp. 361–368.

[4]Miller, D. B., and Bethke, G. W., "Cyclotron Resonance Thruster Design Techniques," *AIAA Journal*, Vol. 4, No. 5, 1966, pp. 835–840.

[5]Kosmahl, H. G., Miller, D. B., and Bethke, G. W., "Plasma Acceleration with Microwaves near Cyclotron Resonance," *Journal of Applied Physics*, Vol. 38, No. 12, 1967, pp. 4576–4582.

[6]Sercel, J. C., "Electron-Cyclotron Resonance (ECR) Plasma Thruster Research," AIAA Paper 88-2916, July 1988.

[7]Kaufman, D. A., and Goodwin, D. G., "Plume Characteristics of an ECR Plasma Thruster," *Proceedings of the 23rd International Electric Propulsion Conference* (Seattle, WA), Vol. 1, Ohio State Univ., Columbus, OH, 1993, pp. 355–360.

[8]Stix, T. H., *Waves in Plasmas*, American Inst. of Physics, New York, 1992, p. 40.

[9]Hooper, E. B., "Plasma Flow Resulting from Electron Cyclotron Resonance Heating on a Magnetic Hill," *Physics of Plasmas*, Vol. 2, No. 12, 1995, pp. 4563–4569.

[10]Hooper, E. B., "Plasma Detachment from a Magnetic Nozzle," *Journal of Propulsion and Power*, Vol. 9, No. 5, 1993, pp. 757–763.

[11]Massey, H. S. W., *Electron Collisions with Molecules and Photo-Ionization, Electronic and Ionic Impact Phenomena*, Vol. 2, Clarendon, Oxford, England, UK, 1969.